Microseismic Case Study: Investigating the Natural Fractures and Faults of the Muskwa & Evie Shale Play in Northeastern British Columbia

Jane Ling, MicroSeismic Canada ULC, William Barker, MicroSeismic Inc.*

Summary

In this case study the natural fracture and faulting characteristics of the Muskwa and Evie shale play in Northeastern British Columbia are discussed. The Muskwa is an ideal formation for studying the acoustic effects of hydraulic fracture stimulation as these shales are known to be generally very brittle, producing lengthy linear fractures. The Evie shales have a different characteristic than the Muskwa shales, consisting of variably calcareous siliceous shales (McPhail, 2008). Both of these shales were studied during microseismic monitoring while hydraulic fracture treatments were performed. The recording geometry for this study was a near-surface array operated during hydraulic fracturing for nine horizontal wells, eight of them within the Muskwa Formation and the ninth in the Evie Formation. Two different completion techniques were used, affecting how the rock fractured: perforation and plug and ball and sliding sleeve. The pointset has a dominant 70º fracture azimuth. The focal mechanisms and *b*-values support this trend result. The Muskwa stimulations differ from the Evie stimulations in that the Evie produces shorter, complex fractures with lower *b*-values and lower stimulated rock volume (SRV). The *b*-value calculated for the H well is 2.97 while it is less than 1 for the A well. This indicates that the fractures in the Muskwa are hydraulically induced while the fractures in the Evie are due to fault reactivation. The SRV calculated for the H well in the Muskwa was 5.5 times more than the SRV for the A well located in the Evie.

Introduction

Microseismic imaging is an extremely powerful method to visualize and map hydraulically induced fractures. It also can help determine various characteristics of the formations undergoing stimulation. The microseismic data for this study was recorded during the hydraulic fracturing of nine horizontal wells, eight of them located within the Muskwa Formation and the 9th in the Evie Formation in Northeastern British Columbia. The general trends in the treatments as well as specific well results are discussed, illustrating various characteristics of stimulated fractures. Two out of the nine wells stimulated with the same ball and sleeve completion technique are examined and compared in detail: Well H in the Muskwa along with Well A in the Evie (Figure 1). The characteristics of imaged microseismicity for each of these wells are explored for this completions technique. The *b*-values as well as the discrete fracture network (DFN) and stimulated reservoir volumes (SRV) for each well will be discussed and compared.

Method

Two different completion techniques were used for this project: Perforation and plug and ball and sliding sleeve. Both methods are common completion techniques used for horizontal wells in unconventional formations.

Wells with sliding sleeve completions are the focus of this case study. The ball and sleeve method is an open-hole technique employing multiple mechanically activated sliding sleeve ports and packers placed within targeted sections of the wellbore to provide stage isolation. Different sized balls are dropped when the sleeves open into corresponding sized seats at a target point in the well. Once the balls are properly seated, the flow of fluids are blocked, increasing back pressure causing the sleeve port to open (Maxwell, 2012). This method was used for wells A, 0, B, G, and H: the 0 and A wells had only eight stages, there were twenty stages for the B well; and fifteen stages for the G and H wells (Figure 1).

These completions were passively monitored with a 95 station near-surface array over an area of approximately 29 square kilometers. The array is designed to have high fold and large aperture in relation to the target depth.

Microseismic Results

There is an average fracture length of >1 km for both the north and south side of the pad with a dominant fracture azimuth of 70°. The maximum horizontal stress orientation in this region from the World Stress Map Project (Heidbach 2008) is predominantly 60º-70º, which is congruent with the fracture azimuths. Regional faults and lineaments maintain a primarily NE-SW orientation with a NW-SE secondary orientation. In general, the microseismicity in the heel stages show a more clustered character than for microseismicity in the toe stages. The southern wells show larger amplitude events with higher event density than the northern wells. Over 29,000 microseismic events are located in on this pad (Figure 1).

DOI http://dx.doi.org/10.1190/segam2013-0677.1

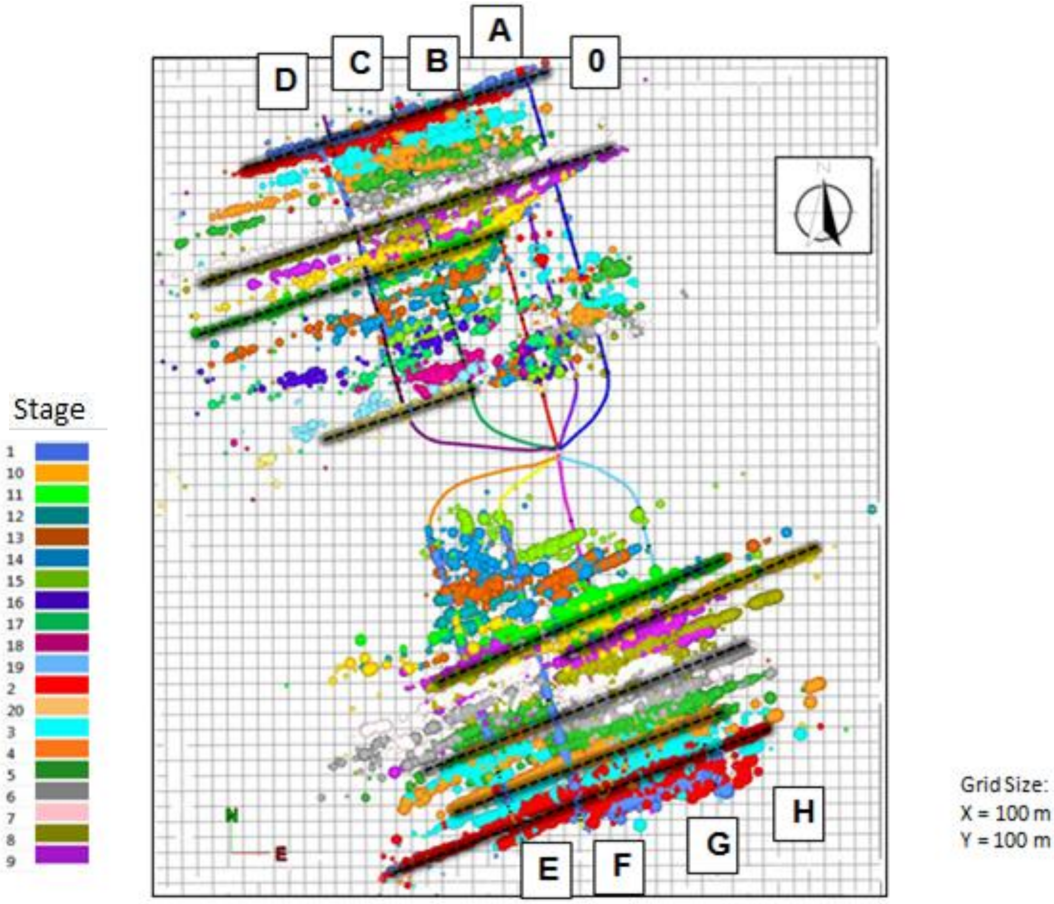

Figure 1: Well field map depicting the well layout and the microseismic events, sized by energy and colored by stage. Microseismic event trends are shown by the dashed lines.

b-values were calculated for each well. A *b*-value is a statistical measure of the relationship between event magnitude and the number of events that occur at that given or greater magnitude. The *b*-value is based on work by the Gutenberg and Richter (Gutenberg & Richter, 1944), shown in Equation 1 where: M is magnitude, and N is the number of events having a magnitude of M or larger. The variables *a* and *b* represent intercept and slope respectively.

$$\mathbf{Log_{10}N = a - bM}$$

Equation 1: The Gutenberg and Richter equation is the basis of b-value calculations in this investigation

In our study the slope, or *b*-value, is determined from the linear portion of the magnitude-frequency relationship. Departures from linear behavior occur at lower and higher magnitudes due to sensor limitations, aperture limitations, and lower event count of higher magnitude events. The purpose of calculating b-values is to distinguish between the types of stress leading to failure during treatment. Event populations with a *b*-value around 2 correlate to hydraulically-induced rock failures while values of approximately 1 are associated with fault reactivation.

A DFN was developed and shows one possible fracture configuration. The fracture size in the DFN is based on an arbitrary but geologically reasonable distribution (Oda, 1985). The fracture orientations are defined using event focal mechanisms, with a statistical scatter applied. The model can be calibrated with rock property data, production data, and additional source mechanism analysis.

The SRV is calculated from the DFN. Every cell containing a non-zero fracture flow property is included in the SRV total. The volumes of cells containing fracture flow properties are summed to obtain a total SRV for this treatment well. The total SRV volume is dependent on the

DOI http://dx.doi.org/10.1190/segam2013-0677.1

size of the model cells and can be adjusted based on known reservoir flow properties.

Well H (Figure 2) shown in light blue, completed in the Muskwa shale, shows well-developed long linear fractures. The planes of these fractures are aligned with the corresponding ball seating location, are well contained, and symmetrical in the lower part of the wellbore. 6,130 events were located for this well. Stage 10, in yellow (Figure 2), shows re-activation of an existing fracture, which extends over 1 km to the east. This large fracture length suggests that NE–SW-trending fractures are reactivated pre-existing natural fractures. There is less microseismicity in the NE part of the well in the later stages as the energy clusters towards the heel of the well. This suggests that there is some sort of structure or stress in the NW-SE direction which inhibits the microseismicity from growing outwards along the NE-SW trend. There is also evidence of later stage energy propagating back into the earlier stages. The *b*-value calculated for the H well is 2.97, indicating that the fractures are hydraulically-induced rock failures (Kratz, et al, 2012). These microseismic trends can easily be seen as they follow the dominant 70° fracture azimuth and create long, linear features. The source mechanism was found to have a strike of 68 degrees, a dip of 86 degrees and a rake of -102 degrees. These values are consistent throughout the well and across the pad. The SRV was found to be 93,414,706 m^3.

Well A (Figure 3) shown in purple, completed in the Evie shale, shows less developed linear fractures than seen in Well H. This well is approximately 500 m deeper than the H well. 254 events were located here. Stages 1 through 6 show microseismicity laterally close to the wellbore with shows some upward growth towards the Muskwa Formation at the toe. Stages 7-8 show microseismicity further west of the wellbore and depicts both upward and downward vertical growth. The lack of clearly defined linear fracture trends may indicate a more complex fracture network being developed within the Evie. The Evie appears to be more structurally controlled than the Muskwa as the microseismicity are more clustered and do not express the linear fracturing seen in Well H.

Three different source mechanisms were located on the A well, two of which are different than those identified for Muskwa stages. The additional source mechanisms were found to have a strike of 349 degrees, a dip of 88 degrees and a rake of 86 degrees and the other to have a strike of 325 degrees, a dip of 84 degrees and a rake of -76 degrees. This supports the interpretation that there are fractures oblique to $S_{Hmax.}$ These may be attributed to fault reactivation instead of hydraulically induced fractures. This is supported by *b*-values less than 1. The SRV (Figure 4) was found to be 17,091,648 m^3. This is about 5.5 times less than the SRV in the H well.

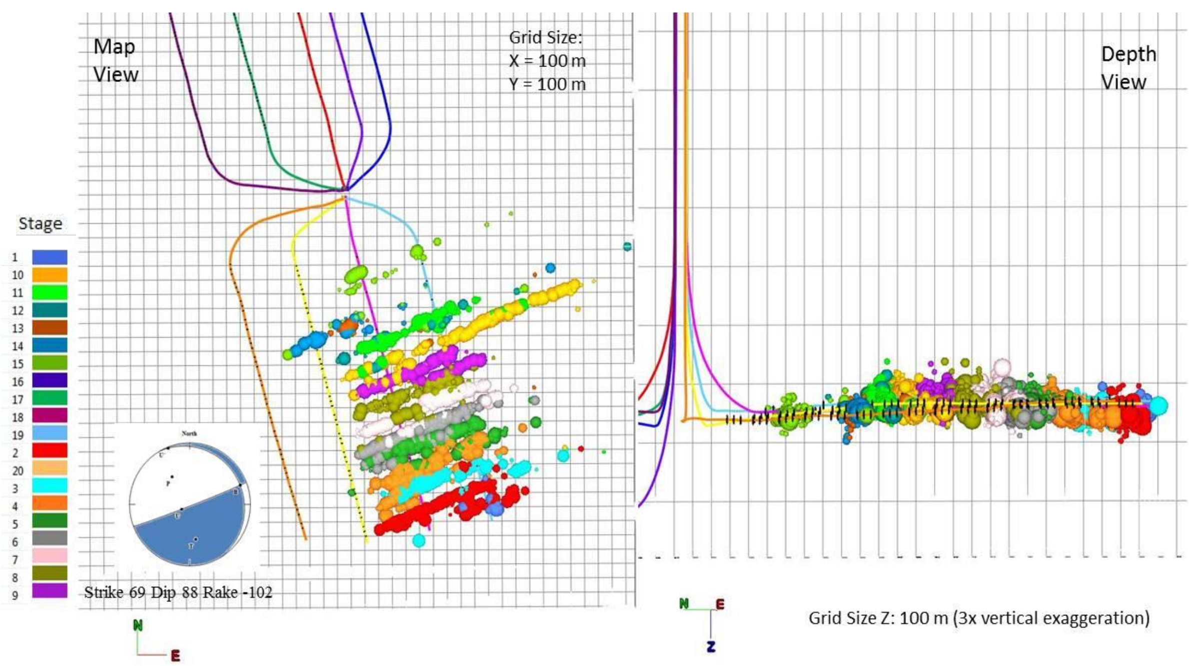

Figure 2: Well H, ball and sliding sleeve completions in the Muskwa formation in both map view (left) and depth view (right) showing the microseismic events sized by energy and colored by stage. Inset in the left picture is the source mechanism beach ball for the well.

DOI http://dx.doi.org/10.1190/segam2013-0677.1

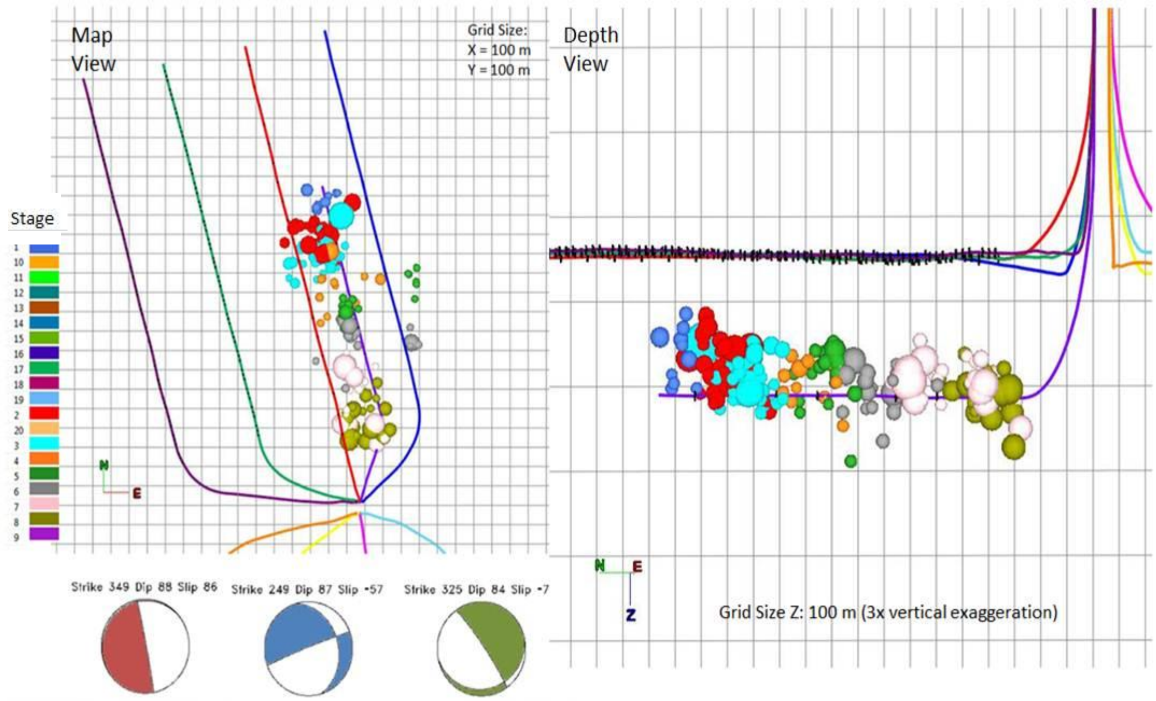

Figure 3: Well A, ball and sliding sleeve completions in the Evie formation, both map view (left) and depth view (right) showing the microseismic events sized by energy and colored by stage. Inset on the left are the source mechanism beach balls for this well.

Well	H	A
Total Fracture Surface Area (m^2)	11,182,100	467,542
Total Fracture Volume (m^3)	24,592	1009
Stimulated Rock Volume (m^3)	93,414,706	17,091,648
Average SRV/stage (m^3)	6,227,647	2,136,456

Figure 4: Table of Total fracture surface area, fracture volume, SRV and normalized average SRV for H and A wells.

The total fracture surface area, fracture volume, SRV, and average SRV/stage were calculated from the microseismic pointsets (Figure 4). The total fracture surface area is double the sum of fracture length multiplied by fracture height. The total fracture volume is the sum of fracture void space in the volume, calculated from fracture areas and apertures. SRV is the volume of geocellular cubes that possess open fracture properties (the affected rock matrix) (Williams-Stroud, S. C. & Eisner, L., 2011).

Conclusions

In this case study, we review an example of the natural fractures and faulting characteristics of the Muskwa and Evie Formations in Northeastern British Columbia. The microseismic pointset displays distinct growth characteristics and trends across the whole pad in the Muskwa Formation. There is a dominant fracture azimuth of 70° for the reactivated natural fractures. The focal mechanisms and *b*-values support this trend result. The total fracture surface area, fracture volume, total SRV, and the average SRV per stage from the microseismic events were also computed for further analysis and comparison. The Muskwa stimulations differ from the Evie stimulations in that the Evie produces shorter, complex fractures with lower *b*-values and lower SRV. This microseismic pointset allows differences and similarities to be examined, which can aid in the planning of future drilling and completions in the Muskwa and Evie Formations.

Acknowledgments

We give a special thanks to the operator for supplying the microseismic results and for helping make this abstract possible. We would also like to thank Paige Snelling for assistance in interpreting the microseismic results.

DOI http://dx.doi.org/10.1190/segam2013-0677.1

http://dx.doi.org/10.1190/segam2013-0677.1

EDITED REFERENCES

Note: This reference list is a copy-edited version of the reference list submitted by the author. Reference lists for the 2013 SEG Technical Program Expanded Abstracts have been copy edited so that references provided with the online metadata for each paper will achieve a high degree of linking to cited sources that appear on the Web.

REFERENCES

Gutenberg, B., and C. F. Richter, 1944, Frequency of earthquakes in California : Bulletin of the Seismological Society of America, **34**, 185–188.

Heidbach, O., M. Tingay, A. Barth, J. Reinecker, D. Kurfeß, and B. Müller, 2008, World stress map: GFZ Hemholtz Center.

Kratz, M., A. Aulia, and A. Hill, 2012, Identifying fault activation in shale reservoirs using microseismic monitoring during hydraulic stimulation: Source mechanisms, b values, and energy release rates: CSEG Recorder, **37**, http://csegrecorder.com/articles/view/identifying-fault-activation-in-shale-reservoirs-using-microseismic-monitor, accessed 21 June 2013.

Maxwell, S., Z. Chen, I. Nizhous, R. Parker, Y. Rodionov, and M. Jones, 2012: Microseismic monitoring of ball drops during a sliding sleeve frac: Geoconvention 2012, CSEG/CSPG/CWLS, Expanded Abstracts, http://www.cspg.org/documents/Conventions/Archives/Annual/2012/085_GC2012_Microseismic_Monitoring_of_Ball_Drops.pdf, accessed 21 June 2013.

McPhail, S., W. Walsh, C. Lee, and P. A. Monahan, 2008: Shale units of the Horn River Formation, Horn River Basin and Cordova Embayment, Northeastern British Columbia : British Columbia Ministry of Energy, Mines and Resources.

Meehan, D. N., 2010, Completion techniques in shale reservoirs: Baker Hughes Reservoir Blog, http://blogs.bakerhughes.com/reservoir/2010/09/18/completion-techniques-in-shale-reservoirs, accessed 21 June 2013.

Oda, M., 1985, Permeability tensor for discontinuous rock masses: Géotechnique, **35**, 483–495.

Williams-Stroud, S. C., and L. Eisner, 2011, Stimulated fractured reservoir DFN models calibrated with microseismic source mechanisms: 44th U. S. Rock Mechanics Symposium, ARMA, Paper 10–520.